PAPER Special Section on Multi-carrier Signal Processing Techniques for Next Generation Mobile Communications

Study on the OVSF Code Selection for Downlink MC-CDMA

Takamichi INOUE[†a)], **Deepshikha GARG**[†], ***Student Members***, ***and*** **Fumiyuki ADACHI**[†], ***Member***

SUMMARY In downlink MC-CDMA, orthogonal variable spreading factor (OVSF) codes can be used to allow multirate communications while maintaining the orthogonality among the users with different data rates. In this paper, we point out that simple selection of the OVSF codes results in degraded performance. We show that this happens because simple code selection results in power concentration over certain consecutive subcarriers; severe power loss in the received signal occurs when these subcarriers experience a deep fade in a frequency selective fading channel. In addition, we show two effective techniques to avoid the performance degradation: random code selection and frequency interleaving; which technique provides a better performance depends on modulation level, code multiplexing order, and presence of channel coding.

key words: *MC-CDMA, MMSE frequency-domain equalization, OVSF code, frequency-selective fading, frequency interleaving*

1. Introduction

In mobile radio communications, the transmitted signal is scattered by many obstacles located between a transmitter and a receiver, thereby creating a multipath fading channel whose transfer function is not anymore constant over the signal bandwidth. Such a propagation channel is called a frequency-selective fading channel [1]. For high speed data transmission in such a frequency-selective channel, multi-carrier code division multiple access (MC-CDMA), wherein each user's data-modulated symbol to be transmitted is spread over a number of subcarriers using an orthogonal spreading code defined in the frequency-domain, has been attracting much attention [2], [3].

In MC-CDMA, minimum mean square error frequency domain equalization (MMSE-FDE), which provides a good trade-off between orthogonality restoration and noise enhancement, gives a good transmission performance [4], [5]. Further performance improvement can be achieved by some form of error control coding; turbo coding [6] has been found to provide strong error correction capabilities [7].

The demand for multimedia communications with variable data rate transmissions including not only voice but also high speed video transmissions is ever increasing. Multirate communications can be realized with orthogonal variable spreading factor (OVSF) codes [8], [9] that have orthogonality among codes with different spreading factors.

The objective of this paper is to point out that when OVSF codes are used for MC-CDMA downlink, the bit error rate (BER) performance degrades depending on how the codes are selected. In this paper, we show that this is because depending on the code selection, power concentrates over certain consecutive subcarriers and such subcarriers appear periodically. In a frequency-selective fading channel, severe power loss in the received signal occurs when the subcarriers with power concentration fall in deep fades and hence, even with MMSE-FDE, the transmission performance degrades. The performance degradation due to power concentration is severe for small number of users (or small number of orthogonal codes to be multiplexed) compared to the spreading factor. Based on the above observation, we show two effective techniques to avoid the performance degradation: random code selection and frequency interleaving.

The remainder of this paper is organized as follows. The MC-CDMA downlink transmission system model is presented in Sect. 2. Section 3 shows the power distribution among the subcarriers when OVSF codes are used. Sect. 4 describes random code selection and frequency interleaving that uniformly distributes the power over the subcarriers. Computer simulations results are presented and discussed in Sect. 5. Section 6 concludes the paper.

2. MC-CDMA Transmission System Model

The transmitter/receiver structure for MC-CDMA downlink transmission is illustrated in Fig. 1. Unless stated otherwise, transmission data rate is the same for all users (i.e., all OVSF codes with the same spreading factor are multiplexed) in order to clearly understand the problem of power concentration over certain consecutive subcarriers. It is assumed that the number of subcarriers is N_c, the spreading factor is SF, and the number of codes is U.

At the transmitter, a turbo-coded and interleavind binary sequence is transformed into a data-modulated symbol sequence. Then, the data-modulated symbol sequence is serial-to-parallel (S/P) converted into N_c/SF-parallel streams and each symbol in the stream is copied SF times before spreading over SF subcarriers by multiplying with the OVSF code. Then, for each subcarrier, all the code components are added and further multiplied by the common scrambling sequence. Inverse fast Fourier transform (IFFT) is performed to obtain the MC-CDMA signal which is transmitted after the insertion of N_g-sample guard interval (GI).

At the receiver, FFT is performed after GI removal to

Manuscript received May 28, 2004.
Manuscript revised August 19, 2004.

[†]The authors are with the Department of Electrical and Communication Engineering, Graduate School of Engineering, Tohoku University, Sendai-shi, 980-8579 Japan.
a) E-mail: inoue@mobile.ecei.tohoku.ac.jp

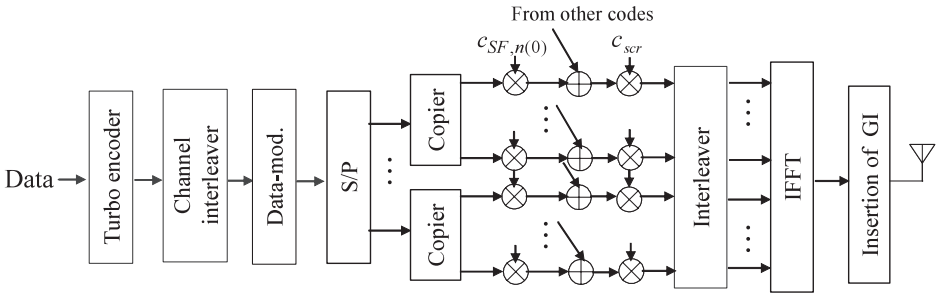

(a) Transmitter.

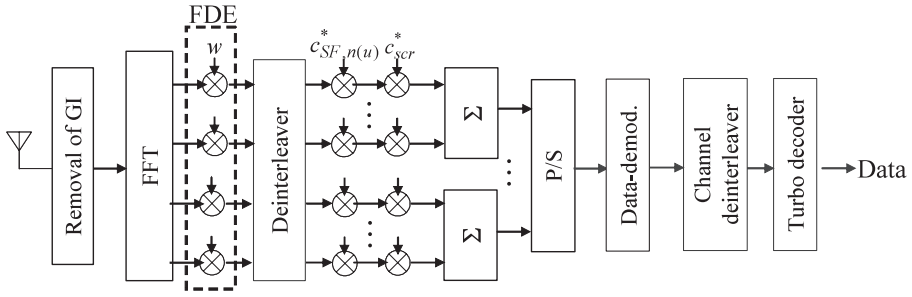

(b) Receiver.

Fig. 1 Transmitter/receiver structure for MC-CDMA downlink transmission.

obtain the N_c subcarrier components. MMSE-FDE is carried out for each subcarrier, followed by frequency-domain despreading over SF subcarriers. After parallel-to-serial (P/S) conversion, soft data-demodulation is carried out to compute the log-likelihood ratio (LLR) for turbo decoding.

3. Performance Degradation due to Power Concentration

3.1 OVSF Code

OVSF codes are generated from a tree structure as shown in Fig. 2 and are Walsh Hadamard codes, but codes appear in a different order. In Fig. 2, the nth code generated from a branch with spreading factor SF is represented as $c_{SF,n}(= \pm 1)$. Any two code sequences with different spreading factors are orthogonal if one of two is not a root (or mother) code of the other.

The spreading pattern when U=16 codes with SF=256 are multiplexed is shown in Fig. 3. It can be observed from Fig. 3 that, when the codes are simply selected from the top, consecutive subcarriers are spread by same spreading chip, resulting in the power concentration over certain subcarriers. The $2n$th code with spreading factor SF is constructed by the concatenation of the nth codes with spreading factor $SF/2$ [8], [9]:

$$\begin{cases} c_{SF,2n} = (c_{SF/2,n} c_{SF/2,n}) \\ c_{SF,2n+1} = (c_{SF/2,n} \overline{c_{SF/2,n}}) \end{cases}, \quad (1)$$

where $\overline{\bullet}$ represents code inversion. Hence, when codes are selected alternately from top, periodic power concentration will appear; the same code pattern appears two times (compare Figs. 3(a) and (b)).

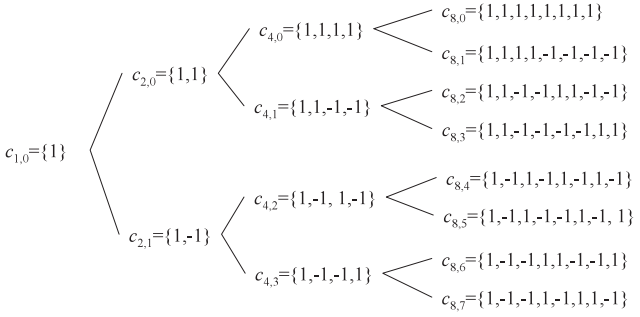

Fig. 2 OVSF code tree.

3.2 Power Concentration

Figure 4 plots the power distribution for SF=256 and U=16 when OVSF codes are used. The power distribution profile for the case when the OVSF codes are simply selected from the top is plotted in Fig. 4(a). It can be seen that when the codes are selected from the top, a power concentration spanning 16 subcarriers appears. Fig. 4(b) plots the power distribution over the subcariers when every alternate OVSF codes are selected from the top (only the even numbered codes are selected). The number of subcarriers over which the power concentration occurs is 8 which is half of that when codes are simply selected from the top. However, the power concentration peak appears twice within the bandwidth. It can be inferred that when the OVSF codes are selected every 2^m codes, power concentration with a width of $SF/(2^m U)$ subcarriers appears. As U increases, the power concentration having narrower width occurs more frequently within the bandwidth, but for the given total power, this leads to

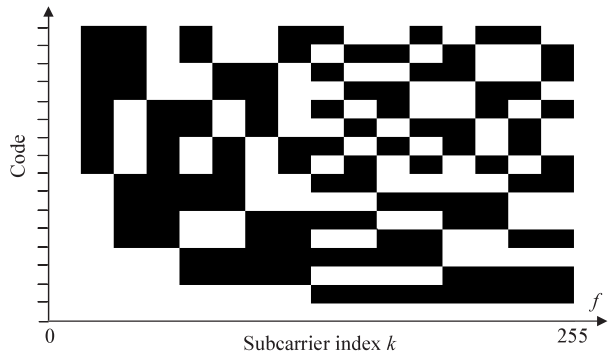

(a) OVSF codes selected from top.

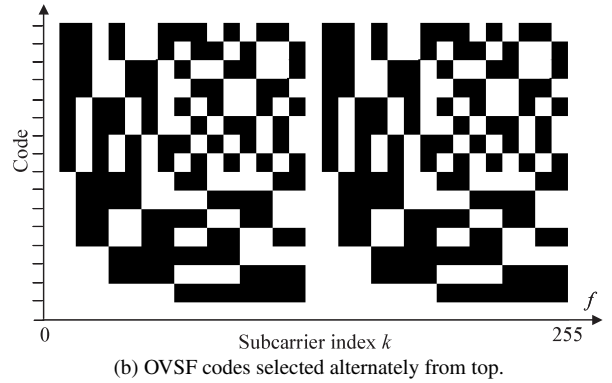

(b) OVSF codes selected alternately from top.

Fig. 3 Spreading code pattern (SF=256, U=16) indicating "white"=1 and "black"= −1.

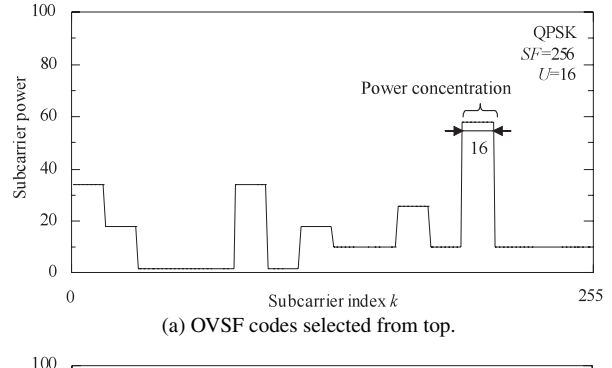

(a) OVSF codes selected from top.

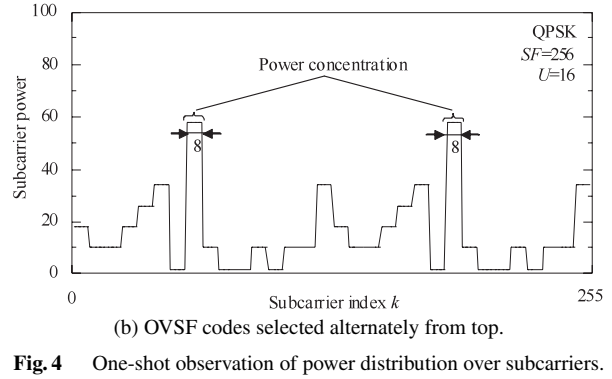

(b) OVSF codes selected alternately from top.

Fig. 4 One-shot observation of power distribution over subcarriers.

uniform power distribution. Hence, the BER degradation, which results due to power concentration, reduces. However, it is not necessary that the code multiplexing order is always high. In this paper, we analyze the extent to which proper code selection of OVSF codes and frequency interleaving can reduce the performance degradation when the code multiplexing order is not high.

3.3 Performance Degradation due to Power Concentration

We assume an L-path frequency-selective fading channel with a time delay separation of Δ samples between adjacent paths. Letting ξ_l be the path gain of the lth path, the channel gain of the kth subcarrier is expressed as

$$H(k) = \sum_{l=0}^{L-1} \xi_l \exp\left(-j2\pi k \frac{l\Delta}{N_c}\right). \tag{2}$$

In this paper, FDE is carried out using the following MMSE weight [3]–[5]:

$$w(k) = \frac{H^*(k)}{|H(k)|^2 + \left(\dfrac{U}{SF}\dfrac{E_s}{N_0}\right)^{-1}}, \tag{3}$$

where E_s/N_0 is the average signal energy per symbol-to-the AWGN power spectral density ratio. FDE and despreading is described in Appendix.

Other equalization weights are maximal-ratio combining (MRC) weight and zero-forcing (ZF) weight (sometimes ZF is called orthogonal restoration combing (ORC)) [2], [3]. The MRC-FDE maximizes the received signal-to-noise power ratio (SNR), but enhances the frequency-selectivity of the channel after equalization. Using the ZF-FDE, the frequency-nonselectivity can be perfectly restored after equalization, but, in turn, the noise enhancement is produced at the subcarriers where channel gain drops. However, the MMSE-FDE can avoid the noise enhancement by giving up the perfect restoration of frequency-nonselective channel. Among various FDE weights, it has been found that MMSE provides the best BER performance. This is because MMSE can provide the best compromise between noise enhancement and suppression of frequency-selectivity. Effect of FDE can be measured by the equivalent channel gain seen after equalization. The equivalent channel gain $\tilde{H}(k)$ is given by $H(k)w(k)$ and becomes

$$\tilde{H}(k) = \frac{|H(k)|^2}{|H(k)|^2 + \left(\dfrac{U}{SF}\dfrac{E_s}{N_0}\right)^{-1}}. \tag{4}$$

The one-slot observation of the channel gain $H(k)$ and the equivalent channel gain $\tilde{H}(k)$ are plotted in Fig. 5. MMSE-FDE gives up the perfect restoration of the channel in order to suppress the noise enhancement. It can be observed that the equivalent channel gain is not flat and there exists a few drops in the equivalent channel gain for the subcarriers falling in deep fades. Furthermore, when the time delay difference between adjacent paths is Δ=2 samples, the deep drop in the equivalent channel gain appears twice. Hence, when the period of the channel gain drop coincides with

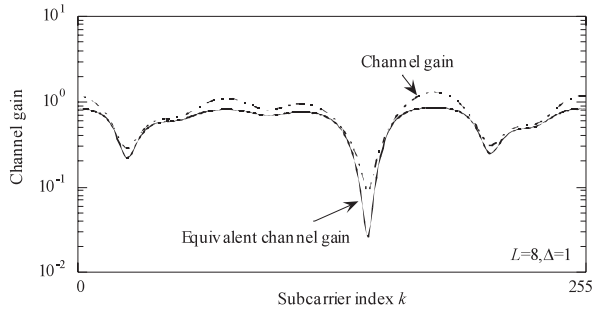

(a) Δ=1.

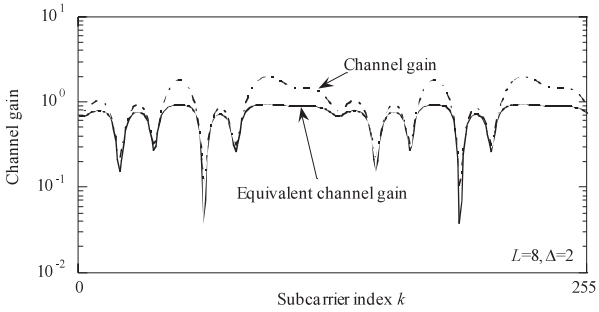

(b) Δ=2.

Fig. 5 Channel gain and equivalent channel gain.

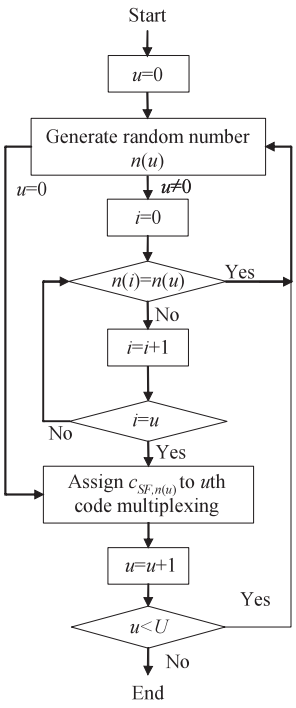

Fig. 6 Flowchart for random code selection.

the period of occurrence of subcarriers with power concentration, the received signal power is reduced and the average BER performance degrades. This is explained in detail in Sect. 5. However, if some technique is introduced to ensure that there is no power concentration over consecutive subcarriers (or the power distribution is uniform over the subcarriers), then the BER performance degradation can be avoided. We will show that random selection of OVSF codes and frequency interleaving are effective techniques to avoid power concentration.

4. Random Code Selection and Interleaving

4.1 Random Code Selection

The flowchart for random code selection is shown in Fig. 6. First, the OVSF code to be used for the uth code multiplexing is selected. A random number $n(u)$ uniformly distributed over $0 \sim SF - 1$ is generated and the $n(u)$th code from the OVSF code tree $c_{SF,n(u)}$ is selected. If the $n(u)$th code has already been allocated, the random number is generated once more. The process is repeated for u=0 to $U - 1$. In this manner, the random selection of OVSF codes is performed.

Figure 7 plots the code pattern and the power distribution over the subcarriers when the codes are randomly selected. The power is distributed almost uniformly over the subcarriers; the periodic nature of power concentration has disappeared.

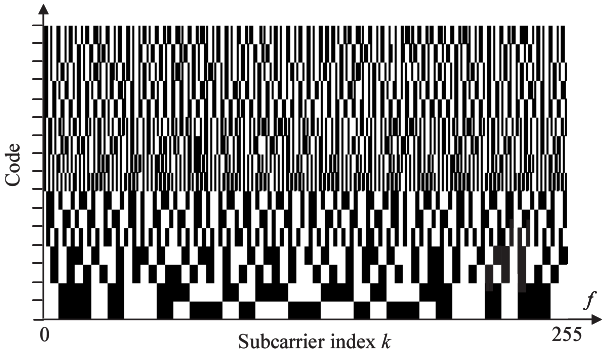

(a) Code pattern indicating "white"=1 and "black"= −1.

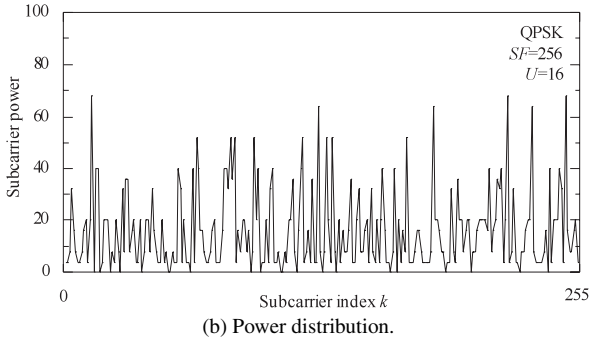

(b) Power distribution.

Fig. 7 Effect of random code selection (SF=256, U=16).

4.2 Frequency Interleaving

The OVSF codes are simply selected from the top and frequency interleaving and de-interleaving are incorporated as shown in Fig. 1. For frequency interleaving, the position of the signal component $S(k)$ at the kth subcarrier position is changed. A random number $R(k)$ uniformly distributed over $0 \sim N_c - 1$ is generated and the subcarrer position of the signal component $S(k)$ is changed such that it is transmit-

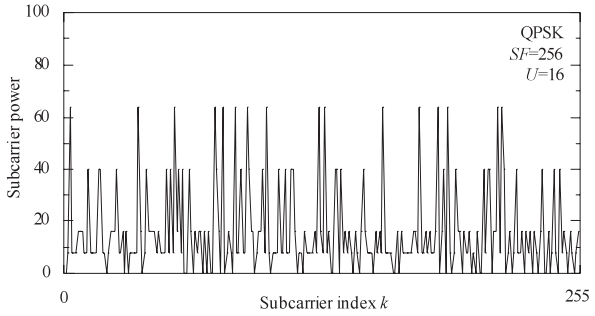

Fig. 8 Power distribution with frequency interleaving (SF=256, U=16).

ted over the $R(k)$th subcarrier. If the subcarrier position $R(k)$ has already been used, another random number is generated. The process is repeated for $k = 0 \sim N_c - 1$ to carry out the frequency interleaving operation.

Figure 8 plots the power distribution over the subcarriers when frequency interleaving is applied instead of random code selection. As a result of frequency interleaving, the transmit power is distributed almost uniformly over the subcarriers, similar to random code selection.

5. Simulation Results and Discussions

Table 1 summarizes the computer simulation conditions. We assume MC-CDMA using N_c=256 subcarriers, GI of N_g=32, and ideal coherent QPSK, 16QAM and 64QAM data-modulations. A frequency-selective Rayleigh fading channel having L=8-path uniform power delay profile is assumed. In the computer simulation, FDE and despreading are carried out as described in Appendix. A rate-1/2 turbo encoder with a constraint length 4 and (13, 15) RSC component encoders with an S-random interleaver [10] is assumed. Log-MAP decoding with 8 iterations is carried out at the receiver. The data sequence length is taken to be K=1024 bits. A 32×64-block interleaver is used as channel interleaver. Ideal channel estimation is assumed.

Table 1 Simulation conditions.

Data Modulation		QPSK, 16QAM, 64QAM
Information bit length		K=1024
Channel interleaver		32×64 block
MC-CDMA	No. of subcarriers	N_c=256
	Guard interval	N_g=32
	Channelization code	OVSF codes (from the top, alternately, random)
	Scrambling code	PN code
	Spreading factor	SF=64, 256
	No. of codes	U=1~64
	Frequency-domain equalization	MMSE
Turbo encoder	Rate	1/2
	Component encoder	(13,15) RSC
	Interleaver	S-random(S=$K^{1/2}$)
Turbo decoder	Component decoder	Log-MAP
	No. of iteration	8
Channel model	Multi path fading	8-path Rayleigh fading
	Delay difference	Δ=1, 2
	Normalized maximum Doppler frequency	$f_D N_c \Delta$=0.001

5.1 Without Channel Coding

Figure 9 plots the effect of the code selection when the time-delay difference is Δ=1 and 2 samples. When Δ=1, the BER performance when the OVSF codes are simply selected from the top is degraded compared to the case when the codes are randomly selected. A possible reason for this is given below. As said in Sect. 3.2, when the OVSF codes are selected in order from the top, a power concentration spanning 16 subcarriers appears once within the bandwidth. However, when the codes are selected alternately from the top (even numbered codes are selected) the power concentration span is over 8 subcarriers which is half of that when codes are simply selected from the top, but this is periodic and appears twice within the bandwidth. Hence, depending on how the codes are selected, the power concentration pattern varies. From this, it is foreseeable that the performance degradation due to code selection depends on the time-delay difference between adjacent paths (i.e., the periodicity in the frequency transfer function of the channel).

When Δ=1, the channel transfer function has one deep fade with a wide fade duration. So, it is more likely that all the subcarriers with power concentration falls within the deep fade. As said earlier, when the subcarriers with power concentration falls in the deep fade, a large power loss in the received signal occurs and, even with MMSE-FDE, theperformance degrades. Hence, the BER performance degradation is the worst. On the other hand, when Δ=2, the fade duration of each deep fade is narrower than that for Δ=1, but is periodic and appears twice. Therefore, the BER degradation is the worst when the codes are selected alternately from the top, which results in two power concentration peaks with a narrower span within the bandwidth. However, with random code selection, the power distribution can be made uniform and the BER performance degradation can be avoided.

Figure 10 compares the BER performance for random code selection and frequency interleaving. Figure 10(a) shows the case when spreading factor is the same as the number of subcarriers (SF=256). For SF=256, frequency diversity gain is high since the data-modulated symbol is spread over all the subcarriers and hence there is no additional performance improvement owing to frequency interleaving. It is seen that the performance is almost the same for frequency interleaving and random code selection. On the other hand, the BER performance for random code selection and frequency interleaving when the spreading factor is less than the number of subcarriers (i.e., SF=64) is plotted in Fig. 10(b). For SF=64, additional frequency diversity gain can be obtained with frequency interleaving, so the BER performance is better than that of random code se-

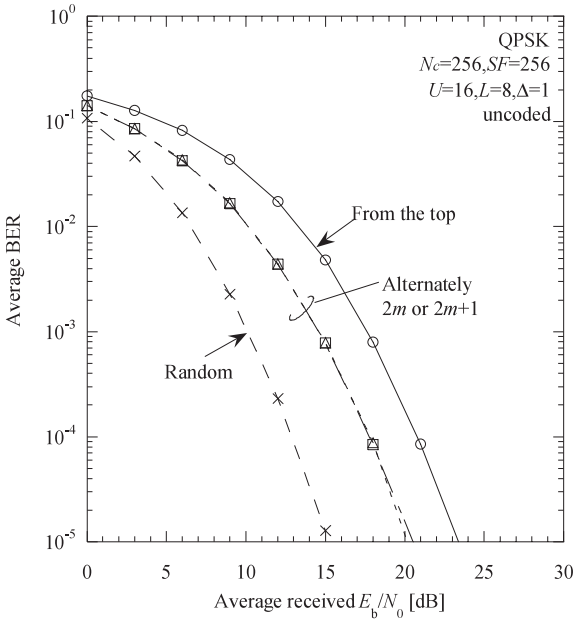

(a) Δ=1.

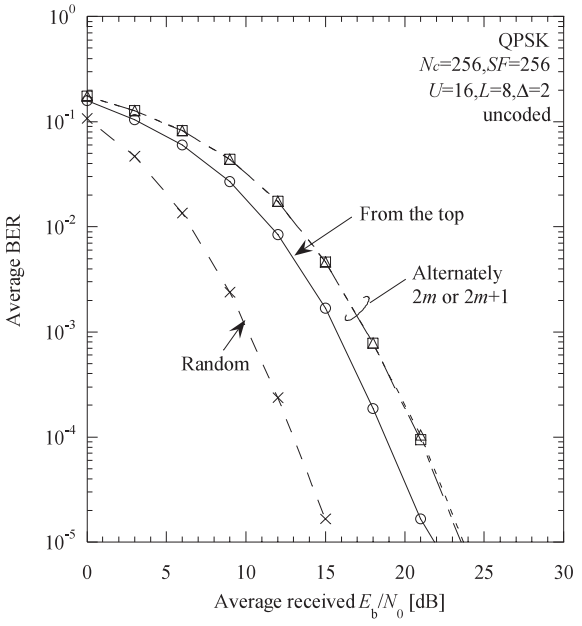

(b) Δ=2.

Fig. 9 Effect of OVSF code selection (without channel coding).

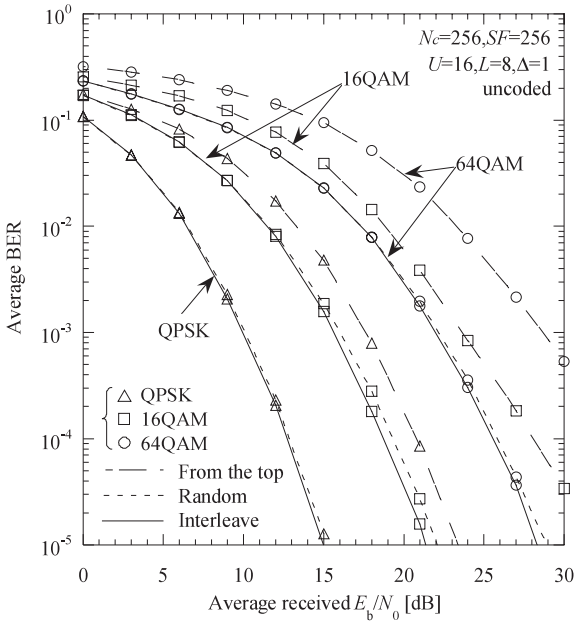

(a) *SF*=256.

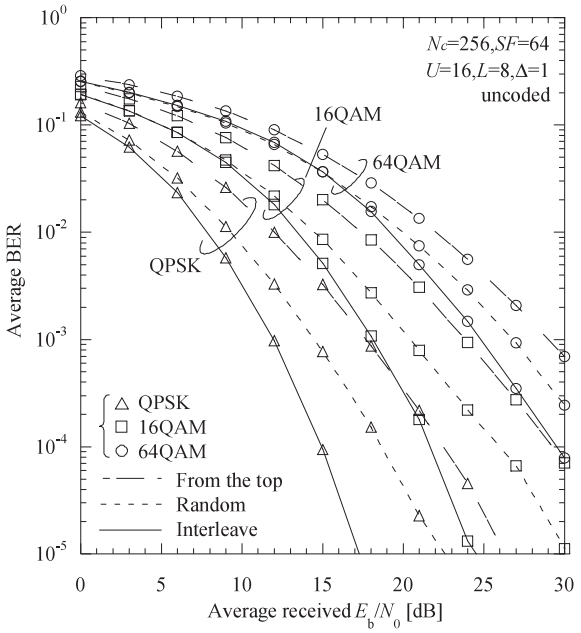

(b) *SF*=64.

Fig. 10 Comparison of random code selection and frequency interleaving for QPSK, 16QAM and 64QAM (without channel coding for U=16).

lection. Hence, it can be said that frequency interleaving provides a BER performance same as or better than that of random code selection.

So far, we have considered the single-rate communication. Here, we discuss the BER performance when multirate users coexist. We consider two classes of users with different spreading factors SF_j (j=0, 1). The number of codes multiplexed within each group is taken to be U_j. Here, we introduce equivalent spreading factor SF_{eq}, defined as $SF_{eq} = \sum_j \frac{U_j}{SF_j}$. Figure 11 plots the BER performance for multirate communications with SF_{eq}=1/4. 8(= U_0) high rate users with SF_0=64 and 32(= U_1) low rate users with SF_1=256 are assumed to coexist. Even for multirate communications, when the codes are selected in order from the top, BER performance degradates because of power concentration as for the single-rate communications. However, random code selection or frequency interleaving can be applied to improve the performance of multirate communications as well.

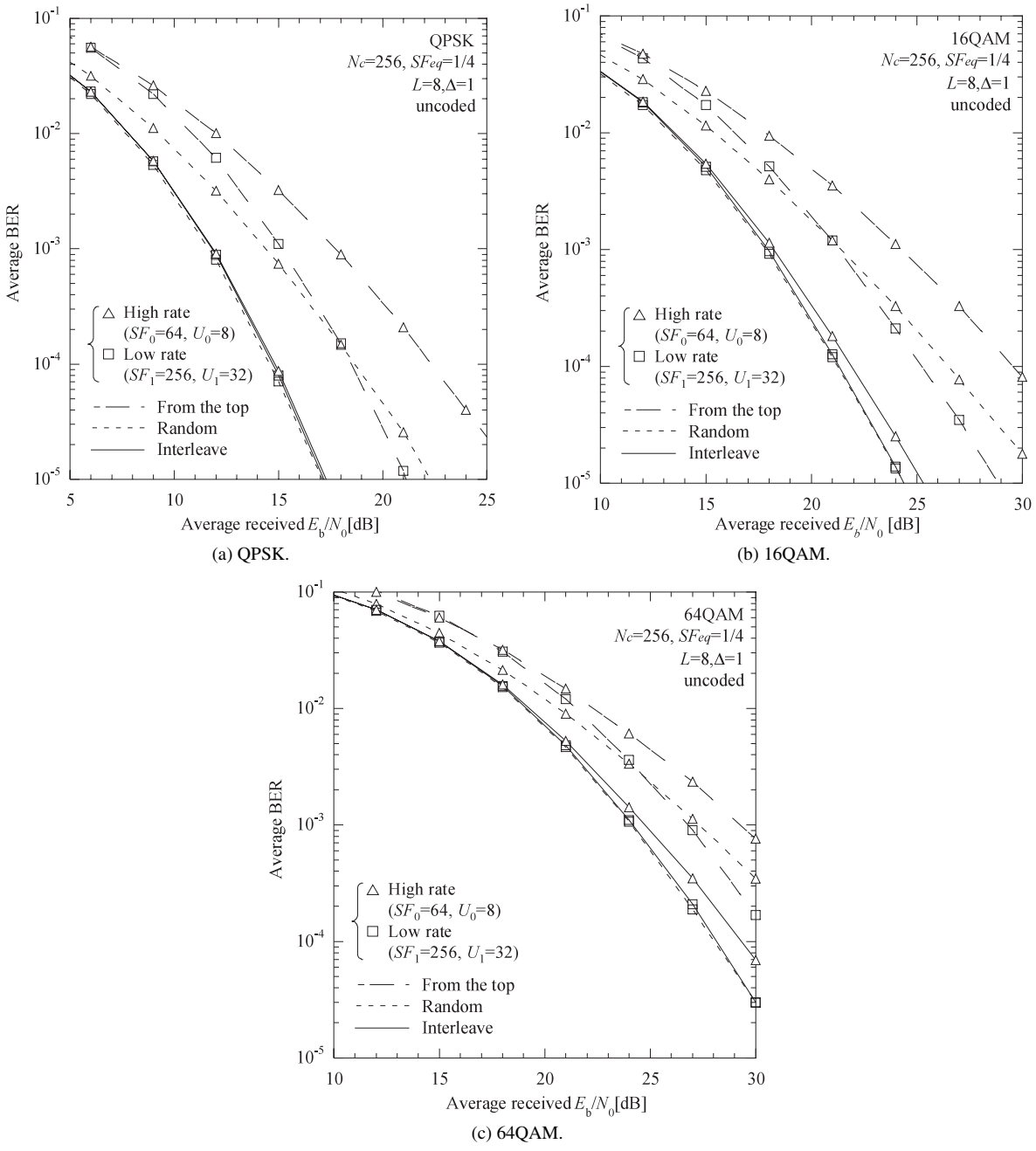

(a) QPSK.

(b) 16QAM.

(c) 64QAM.

Fig. 11 BER performance for multirate communications with SF_{eq}=1/4.

5.2 With Channel Coding

Figure 12 plots the average BER performance for random code selection and frequency interleaving when rate-1/2 turbo coding is applied. For QPSK and 16QAM, frequency interleaving gives a better BER performance than random code selection as for the uncoded case. However, for 64QAM, the BER performance of random code selection is better than that of frequency interleaving. In MMSE-FDE, perfect restoration of the orthogonality is given up to prevent noise enhancement. Hence, the channel transfer function is not completely flat even after MMSE equalization. MMSE weight approaches the MRC weight in the low E_b/N_0 regions, where the effect of noise is more dominant than ICI. Although MRC can maximize the SNR, it enhances the channel frequency-selectivity. Hence, in the low E_b/N_0 regions, there exist deep drops in the channel transfer function even after MMSE equalization. Accordingly, the use of frequency interleaving aids in further increasing the channel selectivity, thus resulting in larger orthogonality destruction among the codes. However, for QPSK and 16QAM, frequency interleaving gives a better performance than random code selection, since QPSK and 16QAM are

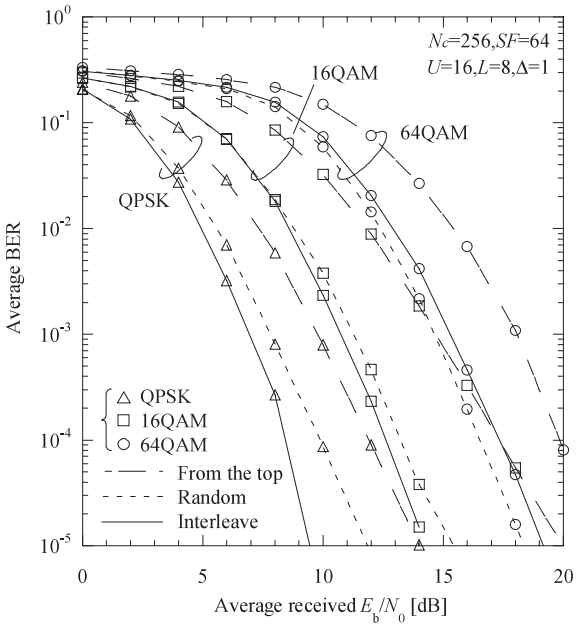

Fig. 12 Effect of random code selection and frequency interleaving for QPSK, 16QAM and 64QAM (with channel coding) when SF=64 for U=16.

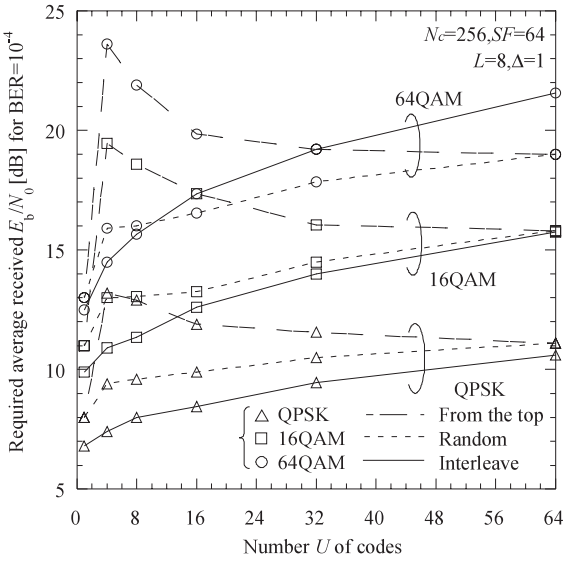

Fig. 13 Required average received E_b/N_0 for a BER = 10^{-4} with channel coding.

less sensitive to orthogonality destruction. On the other hand, for 64QAM, the Euclidean distance between the signal points is shorter and the effect of orthogonality destruction is severe. Therefore, frequency interleaving results in a BER performance worse than that of random code selection. It should be noted that when channel coding is not applied (see Fig. 10(b)), the BER performance of 64QAM is seen to be almost the same for frequency interleaving and random code selection; however frequency interleaving provides a slightly worse BER performance in the low E_b/N_0 regions. The performance difference is not clearly visible for the uncoded case as for the coded case because the BER is around a high value of 0.1.

Figure 13 plots the required average received E_b/N_0 for a BER=10^{-4} as a function of the number U of multiplexed codes. For QPSK and 16QAM, frequency interleaving gives a better performance than random code selection due to higher frequency diversity gain. However, 64QAM is more sensitive to the orthogonality destruction, caused by frequency interleaving, as the code multiplexing order increases. For random code selection, the required average received E_b/N_0 is lower than frequency interleaving when $U > 16$ for 64QAM. It is interesting to note that when the OVSF codes are selected simply from the top, the performance degrades drastically for small U. This is because the power concentration occurs over SF/U subcarriers and this effect is worse when U is smaller; the performance is the worst for U=4. As U increases, the effect of power concentration becomes less, and the performance degradation becomes smaller. The performance degradation due to the power concentration resulting from code selection is worse for higher level modulation.

6. Conclusion

In this paper, we have evaluated the effect of OVSF code selection on the performance of downlink MC-CDMA with and without turbo coding. Simply selecting the OVSF codes from top results in degraded performance. We have shown that this happens as power concentration over consecutive subcarriers is periodic and coincides with the period of the fading drops in a frequency selective channel. Effective techniques to avoid such power concentration are random code selection and frequency interleaving. When channel coding is not applied, frequency interleaving provides a better BER performance than random code selection for all modulation schemes. With channel coding as well, frequency interleaving provides a better performance for QPSK and 16QAM. However, for 64 QAM, the effect of orthogonality destruction is severer and when the number of multiplexed codes is large (e.g., $U > 16$), random code selection is more effective.

References

[1] W.C. Jakes, Jr., ed., Microwave Mobile Communications, Wiley, New York, 1974.
[2] S. Hara and R. Prasad, "Overview of multicarrier CDMA," IEEE Commun. Mag., vol.35, no.12, pp.126–133, Dec. 1997.
[3] T. Sao and F. Adachi, "Comparative study of various frequency equalization techniques for downlink of a wireless OFDM-CDMA system," IEICE Trans. Commun., vol.E86-B, no.1, pp.352–364, Jan. 2003.
[4] A. Chouly, A. Brajal, and S. Jourdan, "Orthogonal multicarrier techniques applied to direct sequence spread spectrum CDMA system," Proc. IEEE GLOBECOM'93, pp.1723–1728, Nov. 1993.
[5] S. Hara and R. Prasad, "Design and performance of multicarrier CDMA system in frequency-selective Reyleigh fading channels," IEEE Trans. Veh. Technol., vol.48, no.9, pp.1584–1595, Sept. 1999.
[6] C. Berrou, A. Glavieux, and P. Thitimajshima, "Near Shannon limit

error-correcting coding and decoding: Turbo codes (1)," Proc. IEEE Int. Conf. Communications, pp.1064–1070, Geneva, Switzerland, May 1993.
[7] J.P. Woodard and L. Hanzo, "Comparative study of turbo decoding techniques: An overview," IEEE Trans. Veh. Technol., vol.49, no.6, pp.2208–2233, Nov. 2000.
[8] F. Adachi, M. Sawahashi, and K. Okawa, "Tree-structured generation of orthogonal spreading codes with different lengths for forward link of DS-CDMA mobile radio," Electron. Lett., vol.33, pp.27–28, Jan. 1997.
[9] K. Okawa and F. Adachi, "Orthogonal forward link using orthogonal multi-spreading factor codes for coherent DS-CDMA mobile radio," IEICE Trans. Commun., vol.E81-B, no.4, pp.777–784, April 1998.
[10] O.F. Acikel and W.E. Ryan, "Punctured turbo codes for BPSK/QPSK channels," IEEE Trans. Commun., vol.47, no.9, pp.1315–1323, Sept. 1999.

Appendix: Frequency-Domain Equalization and Despreading

The low-pass equivalent code-multiplexed kth subcarrier component to be transmitted can be written as

$$S(k) = \sqrt{\frac{2P}{SF}} \sum_{u=0}^{U-1} c_{SF,n(u)}(k \bmod SF) c_{scr}(k) \times x_u\left(\left\lfloor \frac{k}{SF} \right\rfloor\right), \quad (\mathrm{A}\cdot 1)$$

where P is the transmit power per code, $c_{SF,n(u)}(k)$ is the nth OVSF code used for the uth user, $c_{scr}(k)$ is the scrambling code, x_u is the data-modulated symbol for the uth user, and $\lfloor a \rfloor$ denotes the largest integer smaller than or equal to a. N_c-point IFFT is applied to generate the MC-CDMA signal $\{s(t); t = 0 \sim N_c - 1\}$ in the time-domain:

$$s(t) = \sum_{k=0}^{N_c-1} S(k) \exp\left(j2\pi k \frac{t}{N_c}\right). \quad (\mathrm{A}\cdot 2)$$

After insertion of the N_g-sample GI, the resultant MC-CDMA signal $\{s(t); t = -N_g \sim N_c - 1\}$ is transmitted over a propagation channel.

The signal received via an L-path frequency selective fading channel can be written as

$$r(t) = \sum_{l=0}^{L-1} \xi_l s(t - l\Delta \bmod N_c) + \eta(t) \quad (\mathrm{A}\cdot 3)$$

for $t = -N_g \sim N_c - 1$, where $\eta(t)$ is the noise due to additive white Gaussian noise (AWGN). The N_g-sample GI is removed and the N_c-point FFT is applied to decompose the received MC-CDMA signal $\{r(t); t = 0 \sim N_c - 1\}$ into the N_c subcarrier components $\{R(k); k = 0 \sim N_c - 1\}$:

$$R(k) = \frac{1}{N_c} \sum_{t=0}^{N_c-1} r(t) \exp\left(-j2\pi k \frac{t}{N_c}\right) = H(k)S(k) + \Pi(k), \quad (\mathrm{A}\cdot 4)$$

where $H(k)$ is the channel gain and $\Pi(k)$ is noise component due to the AWGN at the kth subcarrier. FDE is carried out as

$$\hat{R}(k) = R(k)w(k) = H(k)w(k)S(k) + \Pi(k)w(k) = \tilde{H}(k)S(k) + \tilde{\Pi}(k). \quad (\mathrm{A}\cdot 5)$$

From comparison of Eqs.(A·4) and (A·5), $\tilde{H}(k) = H(k)w(k)$ is called the equivalent channel gain, given by

$$\tilde{H}(k) = H(k)w(k) = \frac{|H(k)|^2}{|H(k)|^2 + \left(\frac{U}{SF}\frac{E_s}{N_0}\right)^{-1}} \quad (\mathrm{A}\cdot 6)$$

for MMSE-FDE. Then, frequency-domain despreading is carried out.

After P/S conversion, soft-valued received symbol sequence is obtained; the ith received symbol $\hat{x}_u(i)$ is given by

$$\hat{x}_u(i) = \frac{1}{SF} \sum_{k=iSF}^{(i+1)SF-1} \hat{R}(k) c^*_{scr}(k) c^*_{SF,n(u)}(k \bmod SF) = \sqrt{\frac{2P}{SF}} \left(\frac{1}{SF} \sum_{k=iSF}^{(i+1)SF-1} \tilde{H}(k)\right) x_u(i) + \mu_{ICI}(i) + \mu_{AWGN}(i). \quad (\mathrm{A}\cdot 7)$$

The first term represents the desired signal component and the second and third terms are the inter-code interference (ICI) and noise due to AWGN, respectively. $\mu_{ICI}(i)$ and $\mu_{AWGN}(i)$ are given by

$$\begin{cases} \mu_{ICI}(i) = \sqrt{\frac{2P}{SF}} \frac{1}{SF} \sum_{k=iSF}^{(i+1)SF-1} \tilde{H}(k) \times \left(\sum_{\substack{u'=0 \\ \neq u}}^{U-1} c_{SF,n(u')}(k \bmod SF) x_{u'}(i) \right) c^*_{SF,n(u)}(k \bmod SF) \\ \mu_{AWGN}(i) = \frac{1}{SF} \left(\sum_{k=iSF}^{(i+1)SF-1} \Pi(k) w(k) c^*_{scr}(k) c^*_{SF,n(u)}(k \bmod SF) \right) \end{cases}. \quad (\mathrm{A}\cdot 8)$$

Finally, data-modulation is carried out to compute the log-likelihood ratio (LLR) using $\{\hat{x}_u(i)\}$ for turbo decoding.

Takamichi Inoue received his B.S. degree in communications engineering from Tohoku University, Sendai, Japan, in 2003. Currently, he is a graduate student at Department of Electrical and Communications Engineering, Tohoku University. His research interests include diversity and equalization techniques for various access schemes in cellular mobile communication systems.

Deepshikha Garg received her BE degree in Electrical and Communications engineering from Kathmandu University, Nepal in 1998. Currently she is in the Ph.D. program in the department of electrical and communications engineering at Tohoku University, Sendai, Japan. Her research interests include error control schemes and accessing techniques for wireless communications. She was the recipient of the 2002 active research award in radio communication systems from IEICE in 2002.

Fumiyuki Adachi received his B.S. and Dr. Eng. degrees in electrical engineering from Tohoku University, Sendai, Japan, in 1973 and 1984, respectively. In April 1973, he joined the Electrical Communications Laboratories of Nippon Telegraph & Telephone Corporation (now NTT) and conducted various types of research related to digital cellular mobile communications. From July 1992 to December 1999, he was with NTT Mobile Communications Network, Inc. (now NTT DoCoMo, Inc.), where he led a research group on wideband/broadband CDMA wireless access for IMT-2000 and beyond. Since January 2000, he has been with Tohoku University, Sendai, Japan, where he is a Professor of Electrical and Communication Engineering at Graduate School of Engineering. His research interests are in CDMA and TDMA wireless access techniques, CDMA spreading code design, Rake receiver, transmit/receive antenna diversity, adaptive antenna array, bandwidth-efficient digital modulation, and channel coding, with particular application to broadband wireless communications systems. From October 1984 to September 1985, he was a United Kingdom SERC Visiting Research Fellow in the Department of Electrical Engineering and Electronics at Liverpool University. From April 1997 to March 2000, he was a visiting Professor at Nara Institute of Science and Technology, Japan. He was a recipient of IEICE Achievement Award 2002 and was a co-recipient of the IEICE Transactions best paper of the year award 1996 and again 1998. He is an IEEE Fellow and was a co-recipient of the IEEE Vehicular Technology Transactions best paper of the year award 1980 and again 1990 and also a recipient of Avant Garde award 2000.